INSTITUTE OF PHYSICS PUBLISHING SEMICONDUCTOR SCIENCE AND TECHNOLOGY

Semicond. Sci. Technol. **22** (2007) 163–167 doi:10.1088/0268-1242/22/2/028

Recombination activity of manganese in p- and n-type crystalline silicon

D Macdonald[1], **P Rosenits**[1,2] **and P N K Deenapanray**[3]

[1] Department of Engineering, College of Engineering and Computer Science, The Australian National University, Canberra, 0200 ACT, Australia
[2] Now at Fraunhofer Institute for Solar Energy Systems (ISE), Heidenhofstr. 2, D-79110 Freiburg, Germany
[3] Centre for Sustainable Energy Systems, College of Engineering and Computer Science, The Australian National University, Canberra, 0200 ACT, Australia

E-mail: Daniel.Macdonald@anu.edu.au

Received 14 August 2006, in final form 4 December 2006
Published 9 January 2007
Online at stacks.iop.org/SST/22/163

Abstract
Silicon wafers implanted with low doses of manganese were annealed at 900 °C to distribute the Mn throughout the sample volume, and were subjected to carrier lifetime measurements. The Mn centres thus introduced were found to decrease the recombination lifetime in both n- and p-type silicon, although the impact was greater in p-type silicon for resistivities near 1 Ω cm. For both p- and n-type samples, the bulk lifetime decreased approximately in proportion to the Mn implantation dose. Comparison with the known effects of other metals on the carrier lifetime in p-type silicon suggest that Mn is less detrimental than point-like Fe or Cr impurities, but more dangerous than Cu or Ni, which tend to precipitate. In n-type silicon on the other hand, Mn was found to have similar recombination activity to Fe, Ni and Cu.

1. Introduction

Manganese as a trace impurity in crystalline silicon has similar properties to iron and chromium, its neighbours in the periodic table. Like Fe and Cr, it has a moderately high solid solubility limit at typical device processing temperatures, as well as a relatively high diffusivity. This makes it a potentially dangerous impurity during the processing of devices such as solar cells, since it may introduce high concentrations of distributed point-like recombination centres. By contrast, metals from higher groups in the periodic table such as Ni and Cu diffuse much more rapidly at lower temperatures, and tend to precipitate very easily during cooling [1]. They therefore agglomerate at crystal defects such as grain boundaries or surfaces, leading to a reduced recombination activity than if they were evenly distributed. On the other hand, metals from lower groups such as Ti and V diffuse too slowly to penetrate deep into the wafer during processing, and also have much lower solubilities [1].

Despite its potential as a dangerous impurity, there are few reports on the recombination activity of Mn in crystalline silicon. This contrasts with the case of Fe, and to a lesser degree Cr, which have been the subject of numerous studies [2]. This has presumably occurred because Mn is not often considered to be a likely contaminant during either crystal growth or device processing. Manganese, however, often occurs in stainless steel, and in the high-carbon steel wires used for wafer slicing. Although it occurs in such materials at concentrations that are much lower (usually less than 1%) than for either Cr or Fe, this represents a potential pathway for Mn contamination. In fact, manganese has recently been detected by means of x-ray fluorescence microscopy in directionally solidified multicrystalline silicon grown for solar cells [3]. The Mn was found in metal-rich inclusions which also contained other metals such as Fe, Ti, Cr, Zn and Mo. These were thought to originate from foreign particles introduced during feedstock handling or crucible packing, possibly as a result of contact with metal equipment. The particles are believed to partially dissolve during ingot growth, releasing metals into the liquid silicon, which can then be incorporated in point-like form in the solidified ingot. The x-ray techniques used in that study could only detect the remaining undissolved core of the particle, but it is likely that the dissolved Mn and other metals would act as recombination centres. It is therefore of interest

to examine the recombination activity of point-like Mn-related centres in crystalline silicon, which is precisely the purpose of this work.

2. Chemical states of manganese in silicon

There is a quite well-established body of knowledge from electron paramagnetic resonance (EPR), electron spin resonance (ESR) and deep-level transient spectroscopy (DLTS) studies on the structure, charge states and energy levels of Mn-related centres in silicon [4–9]. DLTS studies have also revealed information about the majority carrier capture cross sections of some of these levels [1]. However, it is usually the minority carrier capture cross section which determines the recombination activity of a defect level, meaning that, currently, little is known about the recombination strength of these Mn-related levels. In fact the only previous direct measurements of carrier lifetime in Mn-doped silicon appear to be those of Carlson [10] and Watters and Ludwig [11], performed 50 years ago.

In this work we took care to ensure that the Mn concentration was kept below the solubility limit during annealing, as described in more detail below, thereby avoiding precipitation. We therefore anticipate that the samples prepared in this work will contain interstitial manganese (Mn_i) or substitutional manganese (Mn_s), or a combination of both, since these forms are known to occur in silicon [5, 6]. EPR and DLTS studies have shown that Mn_i has four charge states, leading to three energy levels in the band gap, a double donor at $E_V + 0.27$, a donor at $E_C - 0.43$ and an acceptor at $E_C - 0.12$ eV [1]. Mn_s is thought to introduce a donor and an acceptor level, at $E_V + 0.34$ and $E_C - 0.43$ eV, respectively [1]. This represents a more complicated situation than that occurs for either Fe or Cr, neither of which occupy substitutional sites, and for which only a single level associated with the interstitial form is present in the band gap. These additional levels mean that the dominant Mn_i and Mn_s levels will be determined by the position of the Fermi level, and hence by the doping type and concentration. Under significant carrier injection, the quasi-Fermi levels will also affect the occupation of the various charge states, and so the dominant levels may change from one injection level to another. In addition, like Fe_i and Cr_i, Mn_i has been shown to form pairs with p-type dopant such as B, Al and Ga [1], which each introduce a single donor level in the band gap.

Nakashima and Hashimoto [9] performed DLTS studies on p- and n-type samples. They found that the dominant levels in p-type silicon were the double donor level of Mn_i and the MnB donor level at $E_C - 0.50$ eV. In n-type samples, they observed the single donor and acceptor levels of Mn_i, and a third donor level near mid-gap which they attributed to Mn_s. Other workers have found that the relative amounts of interstitial and substitutional Mn depend on the annealing temperature [12], while others found that the cooling conditions also affected which levels were observed with DLTS [4]. These results show that it is difficult to state *a priori* which Mn-related levels will occur for given experimental conditions. Since DLTS usually only detects levels in the majority-carrier band-half, some levels which are present in high concentrations may go undetected. The purpose of this work is not to identify specific levels, but to measure the impact on carrier lifetime of whichever Mn-related levels are dominant in both n- and p-type silicon after a processing step with a temperature and cooling rate typical for devices such as solar cells. This will enable us to establish the potential danger of Mn contamination in comparison to the known impact of other impurities such as Fe, under realistic processing conditions.

3. Experimental details

The silicon wafers used in this study were float-zone grown with a surface orientation of ⟨1 0 0⟩. The n-type samples were phosphorus-doped with a resistivity of 2 Ω cm ($N_D = 2.4 \times 10^{15}$ cm^{-3}, 200 μm thick), while the p-type samples were boron-doped with resistivities of either 1 Ω cm ($N_A = 1.5 \times 10^{16}$ cm^{-3}, 460 μm thick) or 20 Ω cm ($N_A = 7 \times 10^{14}$ cm^{-3}, 500 μm thick). Prior to Mn implantation, the wafers were etched in a HF/HNO_3 solution to remove surface damage, and then RCA cleaned. Samples of each resistivity and type were then implanted with MnO^- ions at an energy of 70 keV to a dose of either 5×10^{10} or 5×10^{11} cm^{-2} on one side only. The MnO^- ions were extracted using a Cs ion source from a Cu cathode housing containing a pressed mixture of MnO_2 and Ag powders (approximately 8:1 by volume). A bending magnet was used to select only the MnO^- ions, removing any Ag or Cu ions from the ion beam. The implantations were performed through a silicon aperture with dimensions of 30 × 30 mm^2, giving an implanted region of a sufficiently large area for subsequent carrier lifetime measurements.

Following further surface cleaning and native oxide removal, the samples were annealed in N_2 gas at 900 °C for 100 min to distribute the implanted Mn throughout the samples, followed by cooling in air to room temperature. Interstitial Mn has a diffusivity of approximately 1.5×10^{-6} cm^2 s^{-1} at this temperature [1], resulting in a diffusion length of 930 μm for these annealing conditions, significantly greater than the wafer thickness. In the absence of precipitation, this should result in an approximately uniform distribution of Mn throughout the thickness of the wafers, with equivalent average volume concentrations of 1.5×10^{12} or 1.5×10^{13} cm^{-3} for the low and high doses, respectively. Note that the solid solubility limit of interstitial Mn at 900 °C is approximately 6×10^{13} cm^{-3} [1]. This is above the targeted volume concentrations, meaning that precipitation should indeed be avoided. Note also that any lifetime-reducing crystal damage caused by the low doses and energy used here have previously been shown to be effectively removed during such annealing [13]. This allows us to attribute any reduction in carrier lifetime after annealing to the presence of the implanted atoms themselves (in this case either Mn or O). Although at 900 °C the majority of the Mn is likely to be in interstitial form, it is possible that during cooling some of this Mn moves to substitutional sites, as some studies indicate that substitutional Mn has a higher solubility at temperatures near 700 °C [12].

Following annealing, the samples were again etched and cleaned, and then received 70 nm thick plasma-enhanced chemical vapour deposited (PECVD) silicon nitride films on each surface. These films passivate the surfaces for sensitive

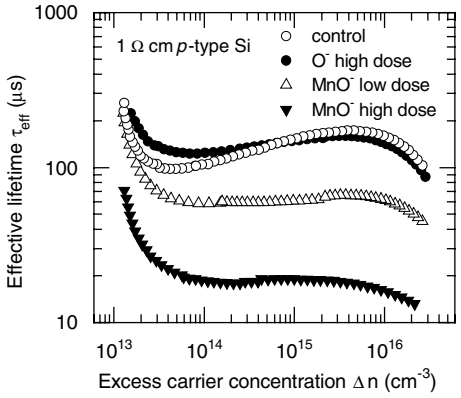

Figure 1. Effective carrier lifetimes as a function of excess carrier concentration for the 1 Ω cm p-type samples.

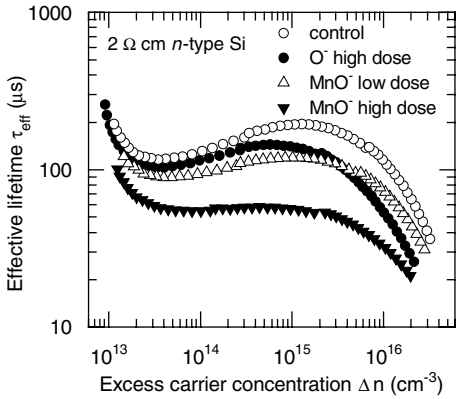

Figure 2. Effective carrier lifetimes as a function of excess carrier concentration for the 2 Ω n-type sample.

measurement of the bulk lifetime. Lifetime measurements were performed with the quasi-steady-state photoconductance technique (QSSPC) [14].

It was necessary to implant MnO^- ions due to the very low yield of Mn^- ions. It is assumed that the MnO molecules break up upon implantation, as occurs in other similar cases, for example implantation of HfO [15]. This results in separated Mn and O atoms in the thin implanted sub-surface region, which are then distributed throughout the wafer thickness by the annealing. Considering that the average O concentration after annealing corresponding to the doses used here is much less than the natural oxygen concentration in this material, the implanted O atoms are not expected to significantly affect the subsequent lifetime measurements. Nevertheless, to check this, another set of samples were implanted with O^- ions alone, extracted from the same cathode as used above. These samples were subject to the same cleaning, etching, annealing and passivation process as the MnO^- implanted samples, in order to reveal any impact of the oxygen atoms on the measured lifetimes. In addition, control samples that received no implantation were also co-processed. These allow the effect of other recombination channels, such as imperfect surface passivation, furnace contamination and native defects or impurities in the starting material, to be assessed.

4. Results and discussion

Figures 1 and 2 show the injection-dependent effective lifetime measurements performed on the 1 Ω cm p-type and 2 Ω cm n-type samples, respectively. The lifetimes are referred to as effective lifetimes because they include recombination channels due to the implanted atoms, as well as due to Auger recombination, surface recombination and recombination through defects native to the starting material or unintentionally introduced during processing. The apparent increase in effective lifetime at excess carrier densities below 10^{14} cm^{-3} is caused by measurement artefacts [16], and does not reflect the recombination lifetime. In order to compare the impact of the implanted impurities on samples of different dopant densities, we have extracted the effective lifetimes at an excess carrier density corresponding to an injection level of $\eta = 0.1$ for the three resistivities studied. These are shown in figure 3. Lower injection levels could not be achieved due to the artefact mentioned above.

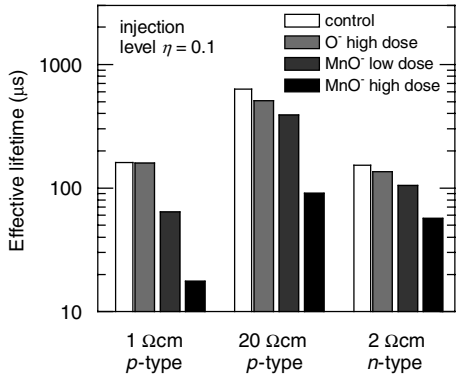

Figure 3. Effective carrier lifetimes extracted at an injection level of $\eta = 0.1$.

As an aside, it is curious to note that for the 1 Ω cm p-type case, the O^- implanted sample is almost indistinguishable from the control, indicating that the presence of the implanted oxygen has almost no impact on this material. On the other hand, the 20 Ω cm p-type and the n-type samples reveal some impact of the oxygen, especially at higher excess carrier densities for the n-type case, as revealed in figure 2.

However, this work is primarily interested in the recombination strength of the Mn impurities. We therefore proceed to extract from the measurements the carrier lifetime due to the Mn impurities alone, τ_{Mn}. For the low dose case, τ_{Mn} is calculated via $1/\tau_{Mn} = 1/\tau_{measured} - 1/\tau_{control}$, where $\tau_{measured}$ is the effective lifetime measured on the implanted sample, and the lifetimes are taken at the same injection level. Here we have assumed that the defects are non-interacting, and that the recombination rates due to each are additive. We have also assumed that the presence of O has a negligible impact for the low dose case. This is certainly true for the p-type case as revealed in figure 1. It is also true for the n-type case considering that the O dose is an order of magnitude less than for the high dose O^- implant shown in figure 2, and at an injection level of $\eta = 0.1$, the impact of the O is negligible even in the n-type case. For the high dose MnO^- implants we have determined the lifetime due to Mn alone via $1/\tau_{Mn} = 1/\tau_{measured} - 1/\tau_{O^-}$, where τ_{O^-} is the lifetime measured on

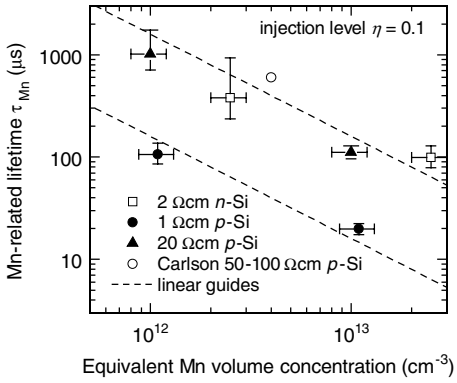

Figure 4. Mn-related lifetimes as a function of Mn concentration (a single point from Carlson also shown).

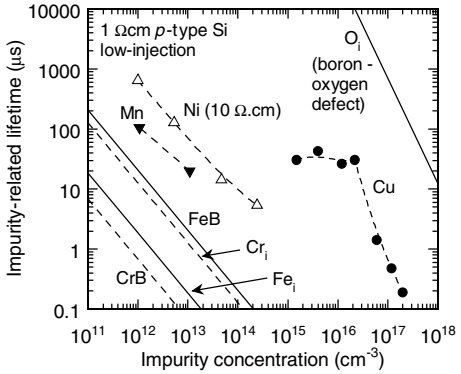

Figure 5. Impurity-related lifetimes in p-type silicon for Mn (this work) and other impurities as taken from the literature. The resistivity is 1 Ω cm (except for Ni, 10 Ω cm), and true low-injection conditions prevail (except for Mn $\eta = 0.1$, Ni $\eta = 0.01$, and B–O $\eta = 0.1$).

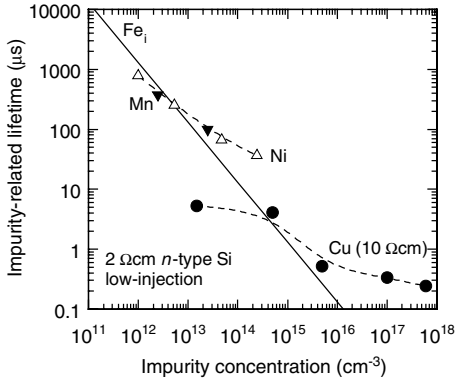

Figure 6. Impurity-related lifetimes in n-type silicon for Mn (this work) and other impurities as taken from the literature. The resistivity is 2 Ω cm (except for Cu, 10 Ω cm), and true low-injection conditions prevail (except for Mn $\eta = 0.1$ and Ni $\eta = 0.01$).

the O^- implanted (high dose) sample. This allows the small impact of the implanted O atoms in the n-type case to be subtracted out.

Figure 4 shows the values of τ_{Mn} calculated in this way. There error bars reflect an estimated 10% uncertainty in the lifetime measurements (the effects of which are compounded when subtracting similar values) and a 20% uncertainty in the equivalent volume dose. The first thing to note is that for all three resistivities studied, the Mn-related lifetime decreases approximately in proportion to the equivalent volume concentration (= implanted dose/thickness). This is precisely what is expected from the Shockley–Read–Hall (SRH) recombination model [17, 18], and serves to indicate that little precipitation has occurred in these samples, as we had intended. The second interesting aspect of the results is that the Mn-related centres clearly have greater recombination strength in the 1 Ω cm p-type material than in the 20 Ω cm p-type or the 2 Ω cm n-type material. Such differences could arise in two distinct ways. First, it is likely that the dominant charge state of the Mn-related centres is different for each resistivity, due to the different positions of the Fermi levels. This can result, for example, in a donor level dominating one type, while an acceptor level dominates the other. It may also be that the Fermi level affects the relative amounts of interstitial and substitutional Mn, with similar consequences. Second, it is possible that even if the dominant type of the Mn-related centre is the same for each resistivity, it can have different recombination properties. This arises because the location of the Fermi level also enters into the SRH model.

Our lifetime results agree well with the value reported by Carlson [10] for 50–100 Ω cm B-doped Czochralski silicon ingots with grown-in Mn. They measured a carrier lifetime of 200 μs where the Mn concentration was estimated to be approximately 4×10^{12} cm^{-3}, at an unspecified injection level. However, this measurement was likely affected by other recombination channels, perhaps the surfaces, as indicated by a measurement of 300 μs in the clean part of the ingot which formed prior to adding Mn to the melt. Treating this second lifetime as a control value and applying the same process described above yields a Mn-related lifetime of around 600 μs, which is the value shown in figure 4.

If there is a significant amount of interstitial Mn in the p-type samples prepared in this work, it is likely that MnB pairs would form. Nakashima and Hashimoto [9] showed that these can be largely dissociated by annealing at temperatures above 250 °C. In analogy to the breaking of FeB pairs [19], such a transformation could result in a dramatic change in carrier lifetime, and may lead to a sensitive method for determining the Mn_i concentration. Annealing our Mn-doped 1 Ω cm p-type sample at 300 °C for several minutes, however, resulted in very little change in lifetime. This may be because the pairs were not dissociated by the annealing, or perhaps the recombination properties of MnB pairs are not very different to the dominant Mn_i level. It may also indicate that there is a significant fraction of substitutional Mn in our samples, which is immobile at room temperature and hence cannot form pairs with dopants.

Finally, it is instructive to compare the lifetimes due to the Mn-related centres, whatever their chemical or charge state, with other known impurities. These are shown in figures 5 and 6 for 1 Ω cm p-type material, and 2 Ω cm n-type material (unless the resistivities are labelled otherwise). In most cases in figures 5 and 6, the data were modelled or measured under true low-injection conditions, meaning that the lifetime has been confirmed to be independent of the injection level, with the exceptions of Mn ($\eta = 0.1$, this work), Ni ($\eta = 0.01$) and the boron–oxygen defect ($\eta = 0.1$). In these cases,

very low-injection conditions could not be reached due to artefacts affecting the photoconductance-based methods for determining the carrier lifetimes. Figures 1 and 2 indicate that there is apparently no strong injection dependence caused by the Mn levels in either n- or p-type silicon, meaning that a comparison with other impurities at lower injection should not lead to large discrepancies.

The results for Fe_i and FeB pairs in figures 5 and 6 are calculated using the SRH model in conjunction with the relatively well-established energy levels and capture cross sections for these defects [20, 21]. Note that these two Fe-related levels result in significantly different lifetimes under low injection in p-type silicon, a phenomenon which has been observed by many authors [20]. The results for Cr_i and CrB pairs are calculated in a similar way. Here we have used the energy levels and cross sections averaged by Graff [1], plus supplementary cross sections as determined from Mishra's [22] capture coefficients and assuming a thermal velocity of 1.1×10^7 cm s^{-1}. As for Fe, these values also result in a significant difference in lifetime between CrB pairs and Cr_i under low injection, although for Cr the pairs are the stronger recombination centre. This has indeed been observed by some authors [22, 23], while others did not find such changes [24], which brings into question the cross sections for these levels. We have therefore not shown Cr_i in the graph for n-type silicon, because the reported variations in capture cross sections cause very large differences in this case. The results shown for Ni and Cu are experimental data from the literature [25, 26], and relate to their precipitates, as these metals are unstable at room temperature in point-like form. Also shown in the p-type case is the boron–oxygen defect that is well known in oxygen-rich Czochralski silicon, and other solar-grade silicon materials [27]. In this case there is a quadratic dependence on the impurity (O_i) content, due to the defect being comprised of an oxygen dimer and substitutional boron.

As shown in figure 5, Mn is significantly less recombination active than the Fe and Cr centres in p-type silicon. Given that the concentration of Mn in steel is usually one or two orders of magnitude lower than Cr and Fe, it seems unlikely to arise as a major lifetime-killing contaminant, unless a specific Mn-rich equipment is used. Note however that Mn is more active than either Ni or Cu. By contrast, in n-type silicon, Fe, Cu, Ni and Mn appear to have similar recombination activity to one another. This activity is reduced in comparison to p-type for Fe, Ni and Mn, but increased in the case of Cu. On balance, n-type silicon is less sensitive to the presence of such metal contaminants, which may be significant for solar cells made with lower grade silicon materials.

5. Conclusion

Manganese surface contamination introduced via ion implantation was found to degrade the bulk lifetime in both n- and p-type silicon wafers after annealing at 900 °C. Although we have not identified the dominant charge state or structural configuration of the resulting Mn-related centres, by keeping the dose below the solubility limit at the anneal temperature, we can at least be confident that precipitation is avoided. The impact of the point-like Mn-related centres on carrier lifetime was significantly greater in p-type material than n-type wafers of comparable resistivity. Compared to the known effects of other metals in p-type silicon, Mn was found to be less harmful than Fe or Cr when they are present in point-like form, but more harmful than Ni or Cu, which occur as precipitates. In n-type silicon, the impact of Mn on carrier lifetime was found to be similar to Fe, Ni and Cu.

Acknowledgments

This work has been supported by the Australian Research Council. The authors are grateful to R Elliman, C Jagadish and H Tan of ANU for access to the ion implantation and PECVD equipment.

References

[1] Graff K 2000 *Metal Impurities in Silicon-Device Fabrication (Springer Series in Material Science* vol 24*)* 2nd edn ed R Hull *et al* (Berlin: Springer)
[2] Weber E R 1983 *Appl. Phys.* A **30** 1–22
[3] Buonassisi T *et al* 2006 *Prog. Photovolt. Res. Appl.* **14** 513–31
[4] Evwaraye A O 1977 *J. Appl. Phys.* **48** 3813–8
[5] Czaputa R, Feichtinger H, Oswald J, Sitter H and Haider M 1985 *Phys. Rev. Lett.* **55** 758–60
[6] Gilles D, Bergholz W and Schröter W 1986 *J. Appl. Phys.* **59** 3590–3
[7] Haider M, Sitter H, Czaputa R, Feichtinger H and Oswald J 1987 *J. Appl. Phys.* **62** 3785–90
[8] Bever T, Emanuelsson P, Kleverman M and Grimmeiss H G 1989 *Appl. Phys. Lett.* **55** 2541–3
[9] Nakashima H and Hashimoto K 1991 *J. Appl. Phys.* **69** 1440–5
[10] Carlson R O 1956 *Phys. Rev.* **104** 937–41
[11] Watters R L and Ludwig G W 1956 *J. Appl. Phys.* **27** 489–96
[12] Gilles D, Schröter W and Bergholz W 1990 *Phys. Rev.* B **41** 5770–82
[13] Macdonald D, Deenapanray P N K and Diez S 2004 *J. Appl. Phys.* **96** 3687–91
[14] Sinton R A and Cuevas A 1996 *Appl. Phys. Lett.* **69** 2510–2
[15] Sachdeva R, Istratov A A, Deenapanray P N K and Weber E R 2005 *Phys. Rev.* B **71** 195–208
[16] Cousins P J, Neuhaus D H and Cotter J E 2004 *J. Appl. Phys.* **95** 1854
[17] Shockley W and Read W T 1952 *Phys. Rev.* **87** 835–42
[18] Hall R N 1952 *Phys. Rev.* **87** 387
[19] Zoth G and Bergholz W 1990 *J. Appl. Phys.* **67** 6764–71
[20] Istratov A A, Hieslmair H and Weber E R 1999 *Appl. Phys.* A **69** 13–44
[21] Macdonald D, Roth T, Deenapanray P N K, Trupke T and Bardos R A 2007 *Appl. Phys. Lett.* submitted
[22] Mishra K 1996 *Appl. Phys. Lett.* **68** 3281–3
[23] Pavelka T 1998 Problems and possibilities of comparing different lifetime measuring instruments and techniques *Recombination Lifetime Measurements in Silicon* vol STP 1340 ed D C Gupta *et al* (West Conshohocken: American Society for Testing and Materials)
[24] Park S H and Schroder D K 1995 *J. Appl. Phys.* **78** 801–10
[25] Sachdeva R, Istratov A A and Weber E R 2001 *Appl. Phys. Lett.* **79** 2937–9
[26] Macdonald D 2005 *Appl. Phys.* A **81** 1619–25
[27] Bothe K, Sinton R and Schmidt J 2005 *Prog. Photovolt. Res. Appl.* **13** 287–96